


## SHORT REPORT

# ***KRAS* mutation-independent downregulation of MAPK/PI3K signaling in colorectal cancer**

Kuen Kuen Lam<sup>1</sup>, Choong Leong Tang<sup>1</sup>, Emile Tan<sup>1</sup>, Siew Heng Wong<sup>2</sup> and Peh Yean Cheah<sup>1,3,4</sup> 

- 1 Department of Colorectal Surgery, Singapore General Hospital, Singapore
- 2 JW Bioscience Pte Ltd., Singapore, Singapore
- 3 Saw Swee Hock School of Public Health, National University of Singapore, Singapore
- 4 Duke-NUS Medical School, National University of Singapore, Singapore

## Keywords

colorectal tumorigenesis; CPTAC; *KRAS* signaling; MAPK/PI3K; SOX9; TCGA

## Correspondence

P. Y. Cheah, Department of Colorectal Surgery, Singapore General Hospital, 20 College Road, The Academia, Discovery Tower Level 9, Singapore 169856, Singapore

Tel: +65 6326 5365

E-mail: cheah.peh.yean@sgh.com.sg

and

S. H. Wong, JW Bioscience Pte Ltd., B1k 226, #10-213, Choa Chu Kang Central, Singapore 680226, Singapore.

Tel: +65 67657696

E-mail: heng@antibodies-targeting.com

(Received 16 September 2021, revised 15 November 2021, accepted 15 December 2021, available online 1 January 2022)

doi:10.1002/1878-0261.13163

*KRAS* is a gatekeeper gene in human colorectal tumorigenesis. *KRAS* is ‘undruggable’; hence, efforts have been diverted to inhibit downstream RAF/MEK/ERK and PI3K/Akt signaling. Nevertheless, none of these inhibitors has progressed to clinical use despite extensive trials. We examined levels of phospho-ERK1/2(T202/Y204) and phospho-Akt1/2/3(S473) in human colorectal tumor compared to matched mucosa with semi-quantitative near-infrared western blot and confocal fluorescence immunohistochemistry imaging. Surprisingly, 75.5% (25/33) of tumors had lower or equivalent phospho-ERK1/2 and 96.9% (31/32) of tumors had lower phospho-Akt1/2/3 compared to matched mucosa, irrespective of *KRAS* mutation status. In contrast, we discovered *KRAS*-dependent SOX9 upregulation in 28 of the 31 (90.3%) tumors. These observations were substantiated by analysis of the public domain transcriptomics The Cancer Genome Atlas (TCGA) and NCBI Gene Expression Omnibus (GEO) datasets and proteomics Clinical Proteomic Tumor Analysis Consortium (CPTAC) dataset. These data suggest that RAF/MEK/ERK and PI3K/Akt signaling are unlikely to be activated in most human colorectal cancer.

## Abbreviations

ACF, aberrant crypt foci; ACTB, beta-actin; Akt, protein kinase B; ANOVA, analysis of variance; Apc, adenomatous polyposis coli; BCA, bicinchoninic acid; COAD, colon adenocarcinoma; CPTAC, clinical proteomic tumor analysis consortium; CRC, colorectal cancer; EGFR, epidermal growth factor receptor; ERK, extracellular signal-regulated kinases; GDC, genomic data commons; GEO, gene expression omnibus; GO:BP, gene ontology:biological processes; GTP, guanosine triphosphate; I.I, integrated intensity; IHC, immunohistochemistry; IκBα, inhibitor of nuclear factor kappa B; kDa, kilo Dalton; KEGG, kyoto encyclopedia of genes and genomes; *KRAS*, kirsten rat sarcoma virus; MAPK, mitogen-activated protein kinase; MCMs, minichromosome maintenance protein complexes; MDC1, mediator of DNA damage checkpoint 1; MEK, MAPK/ERK Kinase; NC, normal crypt; NCBI, National Center for Biotechnology Information; NF-κB, nuclear factor kappa-light-chain-enhancer of activated B cells; NI-WB, near-infrared western blot; PBS, phosphate buffered saline; PDAC, pancreatic ductal adenocarcinoma; PI3K, phosphoinositide 3-kinase; Raf, rapidly accelerated fibrosarcoma; Ras, rat sarcoma virus; SDS/PAGE, sodium dodecyl sulfate/polyacrylamide gel electrophoresis; SOX9, sex-determining region Y-box transcription factor 9; TAK1, transforming growth factorbetaactivated kinase 1; TCGA, the cancer genome atlas; vs, versus; Wnt, wingless and Int-1; WT, wild-type.

## 1. Introduction

Colorectal cancer (CRC) is the world's fourth most deadly cancer with almost 900 000 deaths annually [1]. CRC is usually asymptomatic in early stages and hence frequently diagnosed at the late stages [1]. The 5-year age-standardized observed survival is only 60% and 10% for lymph node involved Stage III and distal organ metastasized Stage IV CRC, respectively [2]. Treatment options for metastasized CRC include chemotherapy, targeted therapy, and immunotherapy. While immunotherapy is a promising development in cancer therapy, majority (~90%) of CRC are microsatellite stable and not amenable to immunotherapy. Currently, the success rate of first-line chemotherapy of 5-Fluorouracil and oxaliplatin for advanced or metastatic CRC is less than 30% [3,4]. Patients who do not respond to this first-line therapy and have wild-type (WT) *KRAS* gene are sometimes given the anti-EGFR (epidermal growth factor receptor)-targeted therapy Cetuximab or Panitumumab. Nevertheless, anti-EGFR treatment is only limited to CRC with WT *KRAS*, the predominant form of Ras in CRC [5]. *KRAS* is a central activator of EGFR signaling. Upon EGFR stimulation, it undergoes activation via GTP exchange mediated by guanine nucleotide exchange factors. *KRAS* oncogenic mutants are resistant to inactivation by GTPase-activating proteins, bypassing the need for continual activation by EGFR. Approximately 50% of CRC harbors *KRAS* oncogenic mutations [6]. Still, patients who receive anti-EGFR treatment eventually develop resistance due to therapy-induced *KRAS* oncogenic mutations driven by natural selection [7,8]. Oncogenic RAS has been shown to be essential for tumor maintenance and *KRAS* mutation in CRC is associated with metastasis and poor prognosis [9–12].

Given its important role in CRC progression, *KRAS* is an obvious therapeutic target. Unfortunately, direct inhibition of *KRAS* is exceptionally challenging as it is not receptive to inhibitor docking [13,14]. To date, the only approved direct *KRAS* inhibitor is Sotorasib (AMG 510) which specifically targets *KRAS* G12C in non-small-cell lung carcinoma by forming a covalent bond with the cysteine [15]. Nevertheless, *KRAS* G12C mutations are rare in CRC. Alternative strategies like inhibition of farnesyl transferase which prevents *KRAS* C-terminal prenylation, required for inner plasma membrane localization where *KRAS* functions, were unsuccessful as farnesyl transferase are functionally replaced by geranylgeranyl transferase [16,17]. Efforts were then diverted to inhibit *KRAS* downstream targets Raf/MEK/ERK, also known as mitogen-activated protein kinase (MAPK) and PI3K/

Akt [18,19]. Despite extensive efforts in research and clinical trials, none of the Raf/MEK/ERK and PI3K/Akt inhibitors have progressed to clinical use for CRC. In fact, to date, only one clinical trial (NCT02788279) has progressed past Phase 2 (reviewed by Xie *et al.* [20]).

The discrepancy of the MAPK and PI3K inhibitor preclinical studies using CRC cell lines and clinical trials outcome led us to question whether MAPK/PI3K signaling is commonly upregulated in human CRC with *KRAS* mutations. As most preclinical trial research of MAPK/PI3K signaling was performed on CRC cell lines and mouse models, they may not emulate the condition in human CRC. Most importantly, we are interested in the extent of activation of MAPK/PI3K signaling in human CRC tumor compared to the corresponding morphologically normal matched mucosa.

## 2. Methods

### 2.1. Study samples

Tumor and matched mucosa samples from resected colon of CRC patients were collected between 2007 and 2017, snap-frozen in liquid nitrogen, and stored in  $-80^{\circ}\text{C}$  in the Department of Colorectal Surgery Tissue Repository, Singapore General Hospital, with written informed consent. Samples used in this study had paired morphologically normal mucosa at least 10 cm away from the tumor. A total of 33 pairs of CRC tumor and matched mucosa tissues were used, which includes tumor with *KRAS* WT ( $n = 8$ ), G12D ( $n = 8$ ), G12V ( $n = 9$ ), G13D ( $n = 5$ ), and others ( $n = 3$ ). The clinico-pathological characteristics of the samples are summarized in Table S1. The study methodologies conform to the standards set by the Declaration of Helsinki and are approved by the SingHealth Centralised Institutional Review Board (CIRB project number 2018/2837).

### 2.2. PCR amplification and sequencing of *KRAS* coding sequences

*KRAS* Exons 2, 3, 4 harboring the coding sequence were PCR amplified from patient genomic DNA using GoTaq® Flexi DNA Polymerase Kit (Promega, WI, USA). The PCR products were purified by isopropanol precipitation. Sequencing was performed with Applied Biosystems (MA, USA) BigDye™ Terminator v3.1 Cycle Sequencing Kit using the PCR products as templates. The reaction was purified by ethanol precipitation and resuspended in Hi-Di™ Formamide and then

separated by capillary electrophoresis in 3500 Genetic Analyzer (Applied Biosystems). The output sequencing results were visualized on Chromas v2.6.4 (Technelysium Pty Ltd, South Brisbane, Australia) as chromatograms and visually inspected for mutations. Both PCR and Sanger sequencing reaction were performed on Biometra (Analytik Jena AG, Jena, Germany) UNOII or GeneAmp 9700 (Applied Biosystems) Thermocyclers. All primers are listed in Table S2.

### 2.3. Protein extraction and concentration reading

Tumor tissues were enriched for neoplastic cells (at least 90%) by macro-dissection while mucosa were used directly after slicing. For protein extraction, tissues were lysed in Tissue Protein Extraction Reagent (T-PER™) supplemented with Halt™ protease and phosphatase inhibitor cocktail (Thermo Fisher Scientific, MA, USA), homogenized with a micro pestle driven by a cordless pestle motor. Protein concentrations were taken with the Pierce™ BCA Protein Assay Kit (Thermo Fisher Scientific) with BSA as standards.

### 2.4. SDS/PAGE and NI-WB

For SDS/PAGE, 10 µg of protein lysates were loaded per well for phospho-ERK1/2 / total ERK1/2 and SOX9 / ACTB and 20 µg of protein lysates per well for phospho-Akt1/2/3 / pan-Akt1/2/3. The loaded samples were separated by electrophoresis using a 10% SDS/PAGE gel in 1X Tris/Glycine/SDS Buffer, ran at 30V, 40 min, then 100 V, 2 h. The SDS/PAGE was transferred to nitrocellulose membrane with Bio-Rad (CA, USA) Transblot using a preset program. After transfer, the membranes were briefly rinsed in MilliQ filtered water and air-dried in fume hood for 1 h. Thereafter, the membrane was rehydrated in PBS for 2 min and then incubated in Intercept Blocking Buffer (LI-COR Biosciences, NE, USA) at room temperature for 2 h with gentle orbital shaking (80 r.p.m.). All primary antibodies were diluted in Intercept Blocking Buffer with 0.2% Tween 20. The membranes were incubated with the diluted antibodies at 4–8 °C overnight (~ 16 h) with gentle orbital shaking. For SOX9 / ACTB NI-WB, the membrane was incubated with only diluted anti-SOX9 antibody overnight and then incubated in anti-ACTB antibody in room temperature for 2 h with gentle orbital shaking (80 r.p.m.). After primary antibody incubation, the membranes were washed with PBS with 0.1% Tween 20 for 5 min, total 3 times. The membranes were then incubated in secondary antibodies diluted in Intercept Blocking Buffer with 0.2% Tween 20 at room temperature for 1 h with gentle orbital

shaking (80 r.p.m.). The membranes were washed then with PBS with 0.1% Tween 20 for 5 min, total 3 times, then in PBS 2 times before imaging. The membranes were imaged with the Odyssey imaging system (LI-COR Biosciences). Integrated Intensity (I.I) K counts values with lane background subtraction, representing WB band intensity, correlating with protein abundance, was calculated by the Odyssey software v3 (LI-COR Biosciences). All primary and secondary antibodies and their corresponding dilutions are listed in Table S3.

### 2.5. Confocal fluorescence immunohistochemistry

Cryosections of 8 µm thickness were prepared from 8 out of the 33 pairs of fresh-frozen CRC tumor and matched mucosa tissues used in NI-WB. Briefly, the cryosections were methanol-fixed and permeabilized. The fixed cryosections were blocked in blocking buffer [5% goat serum, 5% fetal bovine serum, 3% BSA in PBS with calcium and magnesium] and subsequently incubated with Rabbit anti-phospho-ERK1/2 (Thr202/Tyr204) (Cell Signaling Technology, Danvers, MA, USA, cat# 4370) or mouse anti-SOX9 (Sigma-Aldrich, MO, USA, cat# AMAB90795), both diluted 1 : 200. After washing, the cryosections were probed with AlexaFluor 555 goat anti-mouse IgG or AlexaFluor 488 goat anti-rabbit IgG (Cell Signaling Technology cat# 4409 and 4412, respectively), both diluted 1 : 1000. The immunostained cryosections were imaged with Nikon A1 confocal microscope (Nikon, Tokyo, Japan).

### 2.6. Statistics and graph plotting

Comparisons between tumor and matched mucosa were performed with paired *t*-test. Comparisons between tumor of different KRAS and BRAF mutations were performed with unpaired *t*-test with Welch's correction. One-way ANOVA was used to test if any group (i.e., KRAS or BRAF mutation) has a significant difference from others. Linear regression was performed to test the correlation between tumor SOX9 and phospho-ERK1/2 levels from NI-WB. The cutoff *P*-value is  $P < 0.05$  for all analyses. All statistics and graph plotting were performed on the GRAPHPAD PRISM v9.1.2 software (GRAPHPAD Software, CA, USA).

### 2.7. Retrieval and analysis of public domain phosphoproteome, proteome, and transcriptome data

Proteome and phosphoproteome final data metrics were retrieved from National Cancer Institute's

Clinical Proteomic Tumor Analysis Consortium (CPTAC) Colon Adenocarcinoma (COAD) dataset via the LinkedOmics portal ([http://linkedomics.org/data\\_download/CPTAC-COAD/](http://linkedomics.org/data_download/CPTAC-COAD/)) [21]. The dataset consists of 96 pairs of tumor and matched mucosa (details in Table S4). The normalized  $\text{Log}_2\text{FC}$  (fold-change) of phospho-ERK1/2 (MAPK3\_Y204 and MAPK1\_Y187) and SOX9 of Tumor vs Normal (i.e., mucosa) were retrieved from the phosphoproteome and proteome dataset, respectively, and the samples were matched to their corresponding KRAS and BRAF mutation status. Phospho-Akt1/2/3(S473) data were not available from CPTAC. CRC tumor SOX9 mRNA levels were from RNA sequencing data in RSEM (RNA-Seq by Expectation-Maximization) values batch normalized from Illumina RNASeqV2 data were retrieved via cBioPortal (<https://www.cbioportal.org/>) [22,23] from the TCGA Pan Cancer Atlas database.

Transcriptome data were downloaded from The Cancer Genome Atlas (TCGA) Genomics Data Commons (GDC) portal (<https://portal.gdc.cancer.gov/>) and NCBI Gene Expression Omnibus (GEO) data repository (<https://www.ncbi.nlm.nih.gov/geo/>), series GSE95132 [24]. Transcriptome retrieved from TCGA were from 35 pairs of CRC tumor with matched mucosa; tumors were microsatellite-stable with known KRAS mutation status (24 KRAS WT and 11 KRAS mutant) (details in Table S4) [25]. GSE95132 consists of 10 pairs of CRC tumor and matched mucosa, and 5 pairs of aberrant crypt foci (ACF) and matched normal crypts (NCs), all tumors and ACFs harbor KRAS somatic mutations (personal communications with Prof Daniel Rosenberg) [24]. Transcriptome data downloaded from TCGA GDC portal were htseq-count files while data from NCBI GEO GSE95132 were raw RNA sequencing fastq files. Both TCGA transcriptome htseq count files and GSE95132 raw RNA sequencing reads were analyzed on the Galaxy server (<https://usegalaxy.org/>) [26]. In brief, htseq count files from TCGA were directly analyzed with DESeq2 module to generate a list of differentially expressed genes between tumor and matched mucosa [27]. Raw sequencing files from GSE95132 were first mapped to the human genome build hg38 with HISAT2 module and then htseq count reads generated with htseq-count module [28,29]. Similarly, differentially expressed genes between tumor and matched mucosa and aberrant crypt foci (ACF) and normal crypts (NCs) are generated with DESeq2 module from htseq-count files which outputs  $\text{log}_2\text{FC}$  (fold-change) of sample vs control with *P*-value adjusted for multiple testing with the Benjamini–Hochberg procedure [27]. Significantly upregulated genes in CRC tumor vs

mucosa, and ACF vs NCs were fed into DAVID Annotation Tool (<https://david.abcc.ncifcrf.gov/summary.jsp>) [30,31] and g:Profiler (<https://biit.cs.ut.ee/gprofiler/>) [32,33]. The number of input and mapped differentially expressed genes for DAVID and g:Profiler analysis are summarized in Table S5. Output consists of Gene ontology biological process (GO : BP), Kyoto Encyclopedia of Genes and Genomes (KEGG) pathway and REACTOME pathway terms associated with the input genes and the corresponding *P*-values indicating significance of association. Output from DAVID uses Modified Fisher Exact adjusted *P*-value [30,31] and output from g:Profiler uses tailor-made algorithm g:SCS adjusted *P*-value [32,33].

### 3. Results

#### 3.1. Lower phospho-ERK1/2 levels detected in tumor compared to matched mucosa

Despite extensive efforts in research and clinical trials, none of the Raf/MEK/ERK and PI3K/Akt inhibitors have progressed to clinical use for CRC [20]. It is worth noting that most of the earlier studies were performed using KRAS oncogenic mutant cancer CRC cell lines. We hypothesized that the failure in targeting the MAPK (Raf/MEK/ERK) and PI3K/Akt pathways in CRC could be likely due to the fact that both pathways are not activated in primary tumors in CRC. To determine the activation states of the MAPK pathway in primary tumor versus (vs) match mucosa, we performed NI-WB to measure the levels of phospho-ERK1/2(T202/Y204, T285/Y187) in primary tumors vs matched mucosa resected from CRC patients. The protein levels were quantified by calculating the I.I K counts of the 44/42 kDa phospho-ERK1/2 and total-ERK1/2 protein bands. The phospho-ERK1/2 protein levels were internally normalized to total-ERK1/2 protein levels within each sample. Subsequent mention of phospho-ERK1/2 levels refer to protein levels normalized to total-ERK1/2. NI-WB revealed that 25 out of 33 (75.8%) of CRC tumor had lower or equivalent phospho-ERK1/2 compared to their matched mucosa tissues (Fig. 1A,B; Fig. S1). The phospho-ERK1 and phospho-ERK2 levels in tumor are significantly lower than matched mucosa (Fig. 1B). Also, tumor phospho-ERK1 and phospho-ERK2 levels were not significantly different between KRAS mutation status (one-way ANOVA,  $P > 0.05$ ) (Fig. 1C). This indicates that the extent of decrease in tumor phospho-ERK1/2 expression level is not associated with KRAS mutation

status. The tumor phospho-ERK1/2 levels were also not significantly different between Duke's stage A/B and C/D tumors (unpaired two-tailed *t*-test) (Fig. 1D). There is no significant difference in phospho-ERK1 levels between right- and left-sided tumors, but significantly higher phospho-ERK2 in right-sided tumor (Fig. 1E). Confocal fluorescence immunohistochemistry (IHC) study of phospho-ERK1/2 in human CRC-matched mucosa and tumor cryosections show that expression is relatively high in mucosa epithelium while low in tumor (Fig. 1F).

### 3.2. PI3K/Akt pathway activation is similarly not detected in CRC tumor by NI-WB

KRAS mutation is reported to activate PI3K/Akt signaling; it is thus interesting to determine whether the PI3K/Akt pathway is similarly perturbed in primary tumor of CRC. We performed NI-WB of phospho-Akt1/2/3(S473) and pan-Akt1/2/3 on the same 32 pairs of human CRC tumors and matched mucosa; 1 pair was omitted due to protein degradation. The phospho-Akt1/2/3 protein levels were internally normalized to pan-Akt levels within each sample. NI-WB revealed that 31/32 (96.9%) of tumor has lower phospho-Akt1/2/3 compared to matched mucosa (Fig. 2A,B; Fig. S2). The phospho-Akt1/2/3 levels in tumor are significantly lower than matched mucosa (Fig. 2B). Also, the tumor phospho-Akt1/2/3 levels are not significantly different between different KRAS mutation status (one-way ANOVA,  $P > 0.05$ ) (Fig. 2C). This indicates that decrease in tumor phospho-Akt1/2/3 levels is not dependent on KRAS mutation status. The tumor phospho-Akt1/2/3 levels are also not significantly different between Duke's stage A/B and C/D tumors (unpaired two-tailed *t*-test) (Fig. 2D). Tumor phospho-Akt1/2/3 is significantly higher in right-sided compared to left-sided tumor (Fig. 2E).

### 3.3. SOX9 protein is upregulated in most human CRC tumors

It is highly possible that other KRAS effectors in CRC could be affected in the primary tumors since our results showed that MAPK and PI3K/Akt pathways were not found to be upregulated in the primary tumors in CRC. One of the KRAS effectors of interest is SOX9. SOX9 had been previously reported to be part of the EGFR/ERK/SOX9 cascade [34]. Thus, it is interesting to determine whether downregulation of phospho-ERK1/2 observed in this study affects the expression of SOX9 in primary tumors in CRC. We investigated SOX9 protein levels in the same 33 pairs

of human CRC tumors and matched mucosa, 2 tumor samples were omitted due to protein degradation observed in ACTB NI-WB. Unexpectedly, 28 out of 31 (90.3%) tumors have higher SOX9 protein levels (normalized to ACTB) than their matched mucosa (Fig. 3A,B; Fig. S3). SOX9 is significantly higher in pooled tumor than matched mucosa (Fig. 3B). SOX9 was found to be significantly upregulated in KRAS WT and mutant tumors compared to matched mucosa (Fig. 3C). Particularly, KRAS G12D had significantly higher tumor SOX9 than KRAS WT (Fig. 3C). Pooled KRAS mutant tumors SOX9 protein levels are also significantly higher than WT (Fig. 3D). The protein levels of tumor SOX9 are not significantly different between Duke's stage A/B and C/D (Fig. 3E) or between right- and left-sided colon (Fig. 3F). Linear regression analysis showed no significant correlation between tumor SOX9 and phospho-ERK1/2 levels (Fig. 3G). Confocal fluorescence IHC study showed higher SOX9 staining in tumor compared to matched mucosa cryosections, especially in tumor harboring KRAS G12D and G12V mutations (Fig. 3H).

## 4. Discussion

In our study, we quantified phospho-ERK1/2 and phospho-Akt1/2/3 protein levels internally normalized to total-ERK1/2 and pan-Akt, respectively, using the LI-COR system of NI-WB. The NI-WB results showed that the activation states of MAPK and PI3K/Akt is relatively lower in most CRC primary tumors (Fig. 1A,B, Fig. S1 and Fig. 2A,B, Fig. S2), regardless of KRAS oncogenic mutation status. Similarly, confocal fluorescence IHC study also showed lower phospho-ERK1/2 in primary tumor as compared to matched mucosa (Fig. 1F). Interestingly, analysis performed on the phosphoproteomics data provided by the CPTAC-COAD dataset [21] also showed that phospho-ERK1(Y204) and phospho-ERK2(Y187) were significantly lower in tumor than matched mucosa [ $\log_2FC$  (fold-change)  $< 0$ ] regardless of the KRAS mutation status (one-way ANOVA,  $P < 0.05$ ) (Fig. S4). This further supported our results showing that the presence of KRAS oncogenic mutation did not induce upregulation of activated phospho-ERK1/2 in CRC primary tumors.

Our results were in agreement with previous studies reporting decreased MAPK activity of human CRC tumor compared with matched mucosa [35–38]. Hoshino *et al.* [39] reported increased MAPK activation in only 7/34 human colon tumors compared to nontumorous tissues from the same individuals. In Haigis *et al.* [40], all 18 human primary CRC tissues did not

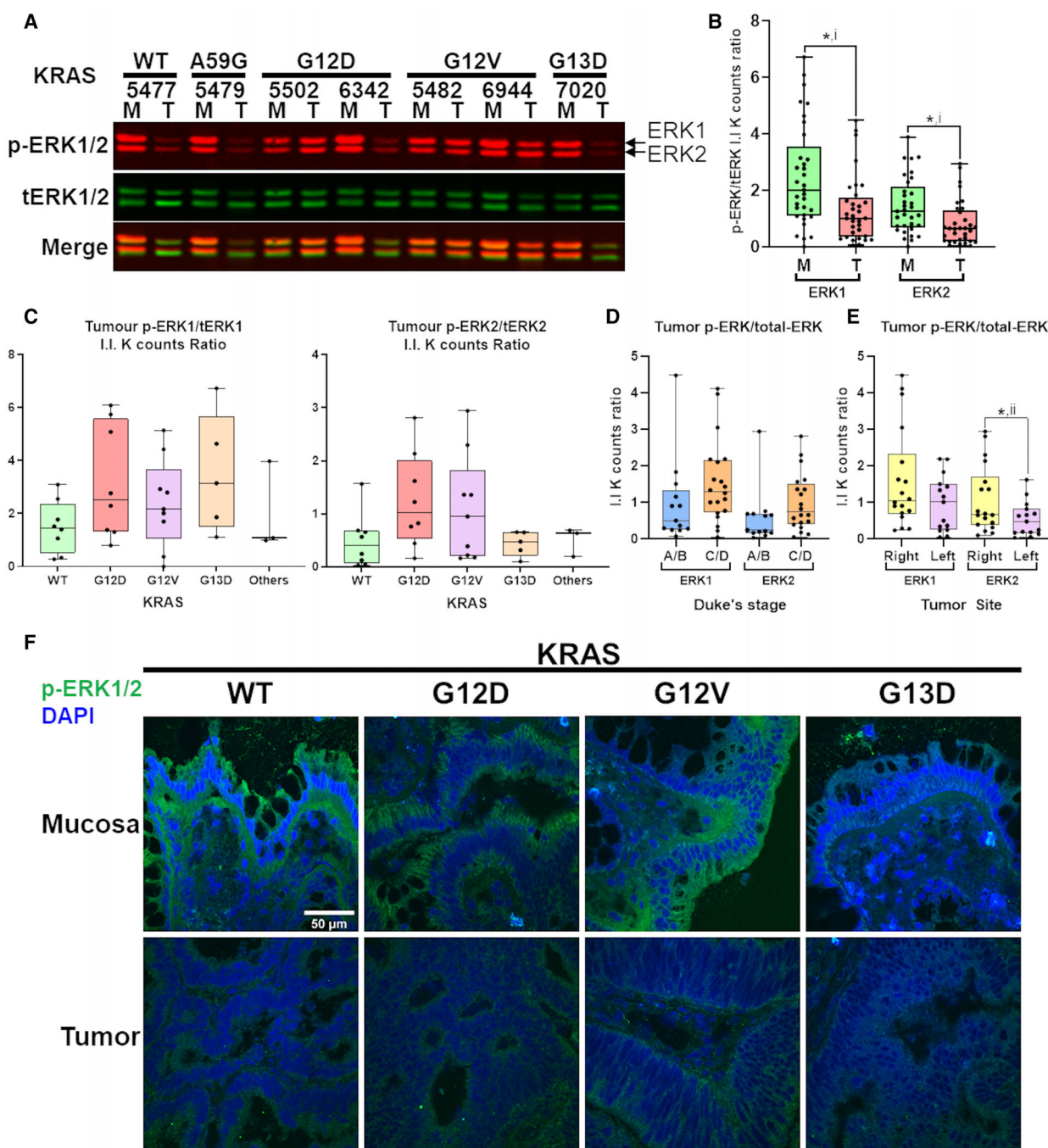


**Fig. 1.** Downregulation of phospho-ERK1/2 in CRC tumor compared to matched mucosa. A representative NI-WB of phospho-ERK1/2 and total-ERK1/2 for 7 pairs of CRC tumor and matched mucosa with tumor *KRAS* mutation status indicated on top (A). Box and whiskers plot of NI-WB phospho-ERK/total-ERK I.I. K counts ratio for ERK1 and ERK2 of pooled mucosa and tumor (B), of tumor grouped by *KRAS* mutation (C), Duke's stage (A/B early stage; C/D advanced stage) (D) and tumor site (right-colon; left-colon) (E). Representative confocal images of phospho-ERK1/2 (green) IHC staining with nuclear DAPI (blue) counterstain of CRC-matched mucosa and tumor cryosections for each *KRAS* mutation status, scale bar = 50  $\mu$ m in top left image is applicable to all images (F). \*two-tailed *t*-test  $P < 0.05$ ; i, paired *t*-test; ii, unpaired *t*-test with Welch's correction. M, mucosa; p-ERK1/2, phospho-ERK1/2; T, tumor; tERK, total-ERK. Both NI-WB (A-D) and IHC (F) were performed on biological replicates ( $n = 33$  and  $n = 8$ , respectively).

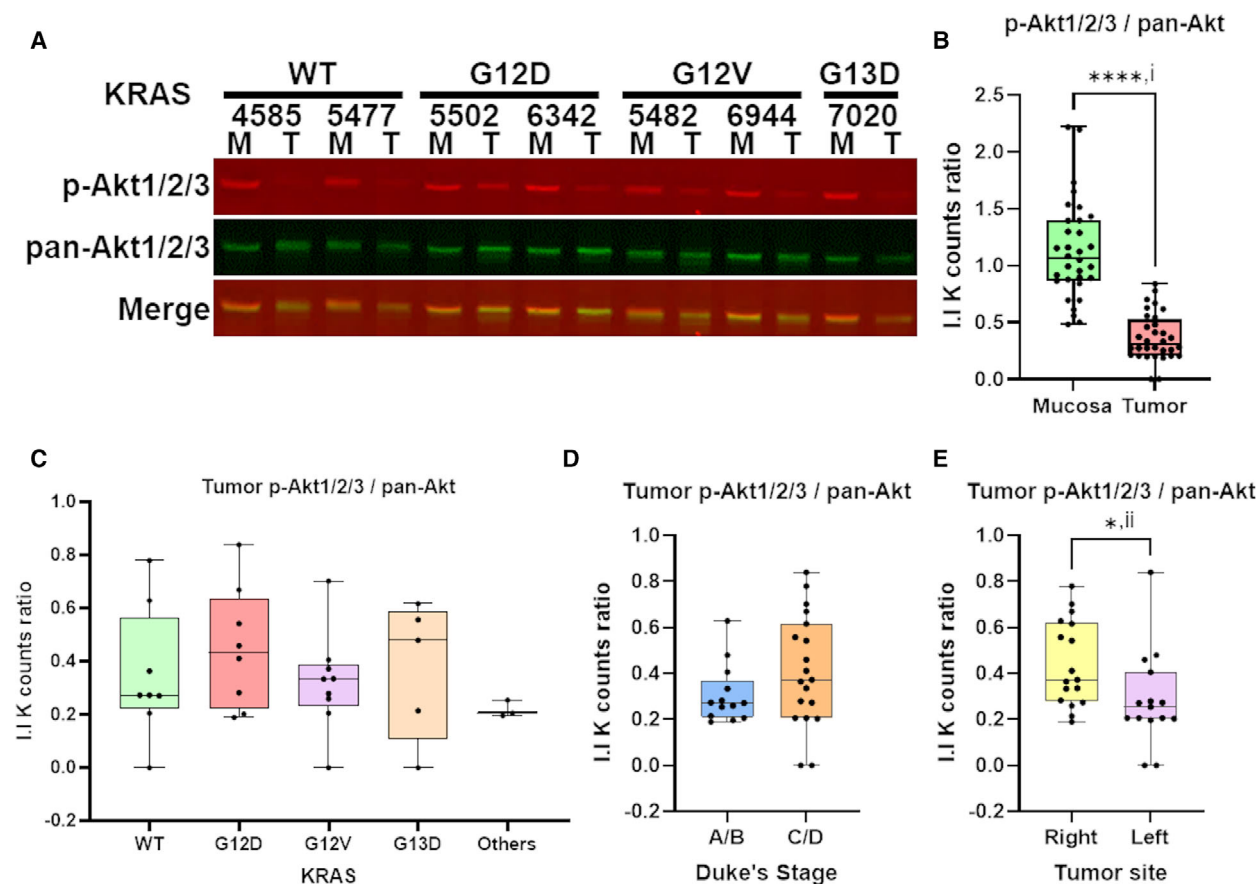
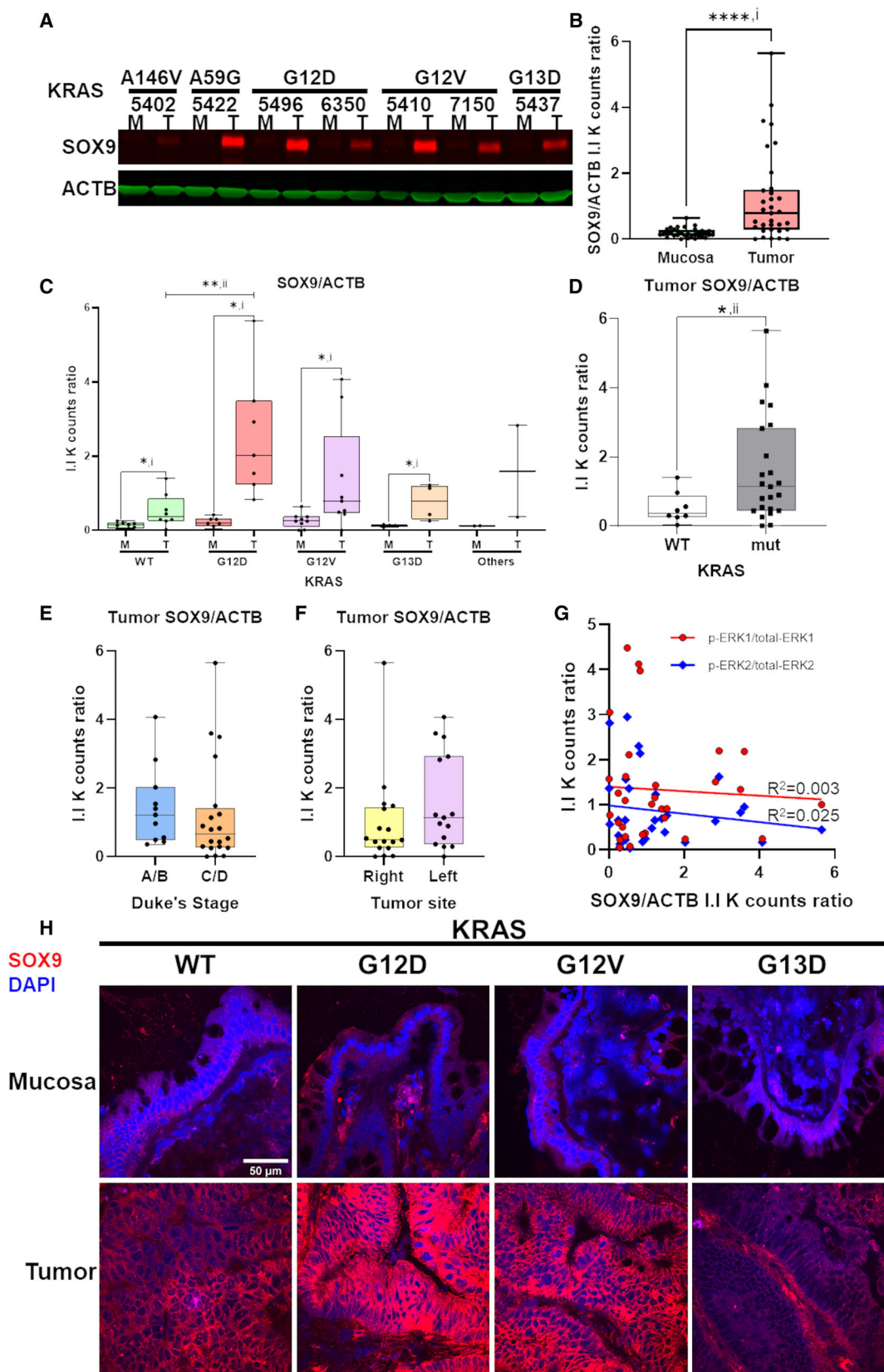


**Fig. 2.** Downregulation of phospho-Akt1/2/3 in CRC tumor compared to matched mucosa. A representative NI-WB of phospho-Akt1/2/3 and pan-Akt for 7 pairs of CRC tumor and matched mucosa with tumor *KRAS* mutation status indicated on top (A). Box and whiskers plot of NI-WB phospho-Akt1/2/3 / pan-Akt I.I K counts ratio of pooled mucosa and tumor (B), of tumor grouped by *KRAS* mutation (C), Duke's stage (A/B early stage; C/D advanced stage) (D) and tumor site (right-colon; left-colon) (E). \*two-tailed *t*-test  $P < 0.05$ ; \*\*\*\*two-tailed *t*-test  $P < 0.0001$ ; i, paired *t*-test; ii, unpaired *t*-test with Welch's correction. M, mucosa; p-Akt1/2/3, phospho-Akt1/2/3; T, tumor. NI-WB (A-D) was performed on biological replicates ( $n = 32$ ).

have positive phospho-ERK1/2 IHC staining while 4 of 18 adjacent mucosa had positive staining. Gulmann et al. [41] reported significantly lower phospho-ERK1/2 in human CRC tumor epithelium compared to matched mucosa epithelium from IHC and western blot experiments. Yeh et al. [42] also reported significantly lower nuclear and cytoplasmic phospho-ERK1/

2 in human CRC tumor epithelium compared to matched mucosa epithelium from IHC of 190 pairs of samples. For studies without mucosa comparison, Sakakura et al. [43] detected MAPK activation in only 4 out of 21 (18%) advanced colon cancer. Schmitz et al. [44] reported positive phospho-ERK1/2 IHC staining in only 20 out of 115 (14.8%) human CRC

**Fig. 3.** *KRAS* mutation-dependent upregulation of SOX9 in CRC tumor compared to matched mucosa. A representative NI-WB of SOX9 and ACTB for 7 pairs of CRC tumor and matched mucosa (A). Box and whiskers plot of SOX9/ACTB I.I K counts ratio of mucosa and tumor pairs from NI-WB ( $n = 31$ ) (B). Box and whiskers plot of NI-WB SOX9/ACTB I.I K counts ratio of mucosa and tumor tissues grouped by tumor *KRAS* mutation status (C), of *KRAS* WT and pooled mutant tumor (D), of tumor grouped by Duke's stage (A/B early stage; C/D advanced stage) phospho-ERK (E) or tumor site (right-colon; left-colon) (F). Linear regression of NI-WB tumor SOX9/ACTB with phospho-ERK1/total-ERK1 or phospho-ERK2/total-ERK2 I.I K counts ratio (G). Representative confocal images of IHC of SOX9 (red) with nuclear DAPI (blue) counterstain of CRC-matched mucosa and tumor cryosections for each *KRAS* mutation status, scale bar = 50  $\mu\text{m}$  in top left image is applicable to all images (H). \*one-tailed *t*-test  $P < 0.05$ ; \*\*two-tailed *t*-test  $P < 0.05$ ; \*\*\*\*two-tailed *t*-test  $P < 0.0001$ . i, paired *t*-test; ii, unpaired *t*-test with Welch's correction. M, mucosa; mut, mutant; T, tumor. Both NI-WB (A-D) and IHC (H) were performed on biological replicates ( $n = 31$  and  $n = 8$ , respectively).





tumors. Altogether, MAPK signaling is rarely activated in CRC tumor. Nevertheless, four studies reported higher tumor MAPK activity compared to matched mucosa [45–48]. While these studies addressed the state of MAPK activation in CRC tumor, there was no association drawn with KRAS mutation status. In our study, we included a substantial number of tumors with common KRAS mutations (i.e., G12D, G12V, G13D); henceforth, revealing that tumor phospho-ERK1/2 levels are not dependent on KRAS oncogenic mutations (Fig. 1C). In agreement, Perkins *et al.* [49] observed no significant difference in phospho-ERK1/2 and phospho-Akt levels between KRAS WT ( $n = 23$ ) and mutant ( $n = 19$ ) CRC tumors, but there was no comparison with mucosa. We only selected samples with matched mucosa at least 10 cm from tumor site to ensure that the mucosa are nontransforming and outside of tumor paracrine influence, providing a suitable basal control. Interestingly, the right-sided tumors have significantly higher phospho-ERK2 (Fig. 1E) and phospho-Akt1/2/3 (Fig. 2E) than left-sided tumors, re-affirming the different cancer biology between right- and left-sided colon [50].

The NI-WB using the LI-COR system allows accurate relative quantification of phospho-ERK1/2 and phospho-Akt1/2/3 levels owing to this system's large dynamic range compared to methods used in previous studies. NI-WB is also more quantitative as phospho-ERK1/2 and phospho-Akt1/2/3 are internally normalized to total-ERK1/2 and pan-Akt, respectively. Importantly, the NI-WB assay revealed high mucosa expression of phospho-ERK1/2 in the matched mucosa (Fig. 1A) suggesting a role in normal colonic homeostasis; targeting phospho-ERK1/2 may thus not be ideal. MAPK and PI3K signaling pathways are crucial in maintaining integrity of tight junctions in normal colonic epithelial cells [51,52]. Thus, high mucosa expression of phospho-ERK1/2 and phospho-Akt1/2/3 is required to maintain integrity (organization) of differentiated epithelial cells in the crypts (Fig. S5, panels A and C). Interestingly, even in the tumors, expression of phospho-ERK1/2 plays a role in determining the organization of crypt's epithelial cells. Higher numbers of collapsed/deformed crypts were observed in primary tumor with downregulated phospho-ERK1/2 expression (Fig. S5, panel B) as compared to primary tumors with upregulated phospho-ERK1/2 expression (Fig. S5, panel D).

While several studies have reported high MAPK activity in CRC cancer cells with KRAS oncogenic mutations, most of them were performed on cell lines or mouse models. Cell lines are highly culture-adapted

and lack the microenvironment of the native tissue, hence unlikely to replicate biological properties of human CRC [53]. Moreover, several studies used phospho-ERK1/2 downregulation as a biomarker to test candidate drug effectiveness on CRC cell lines without a noncancerous control for comparison of MAPK activation. A few studies which assayed MAPK activation in multiple CRC cell lines have vast variability between cell lines. In Hoshino *et al.* [39], only 7/17 CRC cell lines had constitutive MAPK activity. Kress *et al.* [54] described substantial variation of phospho-ERK1/2 levels in 64 CRC cell lines, with 25 high, 18 moderate and 21 low to nondetectable phospho-ERK1/2 levels. Mouse models of CRC have significant differences with human, as well as the method of CRC induction usually involves either chemical (i.e., 1,2-dimethylhydrazine) treatment or pan-colonic *Apc* knockout which is starkly different from human sporadic CRC tumorigenesis which likely arise from random mutation events of a single initiating cell [55,56]. As most preclinical studies of drugs targeting MAPK signaling were performed on cell lines and mouse xenografts of cell lines, they may not be translated into clinical settings [57].

Our results raised the question of how activation of the MAPK/PI3K signaling pathways were perturbed in CRC primary tumors as compared to matched mucosa, regardless of the KRAS mutation status. To shine more light on this issue, bioinformatics analyses were performed on transcriptome datasets extracted from TCGA and NCBI GEO series GSE95132 [24]. Results from this analysis showed that upregulated genes in tumor vs mucosa and aberrant crypt foci vs adjacent normal crypts were not significantly associated with MAPK-related and PI3K-related Gene Ontology Biological Processes (GO : BP), KEGG, and REACTOME pathway terms (Tables S6A, S7A). On the other hand, downregulated genes in tumor from both the KRAS WT and mutant TCGA datasets were observed to be significantly associated with 3 MAPK-related and 6 PI3K/Akt-related GO : BP terms (Tables S6B, S7B). Downregulated genes from TCGA KRAS WT but not mutant was significantly associated with the KEGG term hsa04010 : MAPK signaling pathway (Table S6B). Analysis of these downregulated genes related to the MAPK and PI3K/Akt signaling pathways will shed light on how ERK1/2 and Akt1/2/3 were perturbed in CRC primary tumors independent of KRAS oncogenic mutants. Our hypothesis is that this may be related to downregulation of EGFR in CRC tumors as interrogating the CPTAC dataset showed significant KRAS mutation-independent downregulation of EGFR in the tumors compared to the

matched mucosa ( $n = 96$  pairs;  $P < 0.0001$ ). A recent study has also provided evidence that Wnt-signaling could repress MAPK signaling in several mouse cancer models [58].

Notably, our NI-WB results indicated that SOX9 protein is upregulated in the tumor compared to matched mucosa (Fig. 3A,B; Fig. S3), and KRAS G12D or pooled KRAS mutant had significantly higher SOX9 protein levels than WT tumors (Fig. 3C,D). Similarly, confocal fluorescence IHC showed higher SOX9 in tumor compared to matched mucosa, with stronger SOX9 immunostaining in KRAS G12D and G12V tumors (Fig. 3H). In agreement, SOX9 protein levels in the CPTAC-COAD proteome dataset are significantly upregulated in tumors compared to matched mucosa, with significantly higher upregulation in KRAS G12V compared to WT (Fig. S6A) [21]. Analyses of the TCGA and GSE95132 paired tumor-mucosa transcriptome datasets also revealed SOX9 to be significantly upregulated in tumor compared to matched mucosa (Table S8).

Furthermore, TCGA Pan Cancer Atlas dataset ( $n = 435$ ) retrieved via cBioPortal exhibited significantly higher SOX9 mRNA levels in CRC tumors with KRAS mutations compared to KRAS WT (Fig. S6B) [22,23]. This indicates that KRAS mutant CRC is associated with higher SOX9 upregulation, indicating possible activation by oncogenic KRAS signaling. On the other hand, we found no correlation between tumor phospho-ERK1/2 and SOX9 protein levels, indicating that SOX9 is unlikely to be activated by phospho-ERK1/2 via the EGFR-ERK-SOX9 axis as reported in urothelial cancer (Fig. 3G) [34]. Human Protein Atlas IHC also showed intense SOX9 antibody staining in the crypt epithelium of CRC tumor sections (<https://www.proteinatlas.org>) [59–61]. SOX9 is a member of the SOX family of transcription factors containing a high mobility group (HMG) DNA binding domain and a transactivation domain. SOX9 plays a role in several developmental and self-renewal processes. Of note, it is upregulated by Wnt/ $\beta$ -catenin signaling and promotes intestinal stem cell renewal. SOX9 is overexpressed in hepatocellular, breast, bladder, gastric, prostate, ovarian, pancreatic, and colorectal cancer [62,63]. A TCGA study predicted SOX9 to be a possible CRC driver [64,65]. In pancreatic ductal adenocarcinoma (PDAC), another KRAS-driven cancer, SOX9 is a critical mediator of KRAS-induced PDAC initiation of pancreatic acinar cells in mouse model [66]. SOX9 has also been implicated to be upregulated by oncogenic KRAS via activation of TAK1/ $I\kappa B\alpha$ /NF- $\kappa B$  signaling in PDAC, in turn promoting PDAC by upregulation of minichromosome maintenance protein complexes (MCMs) and mediator of DNA damage checkpoint 1 (MDC1) [67].

Taken the evidences together, we propose that SOX9 could be a novel KRAS downstream effector and a potential therapeutic target but further research into its role in CRC is required.

## 5. Conclusions

In conclusion, while MAPK/PI3K signaling is widely accepted to be mitogenic, it is not activated in most CRC tumors regardless of KRAS mutation status. The widespread use of phospho-ERK1/2 as a biomarker in drug testing on CRC cell lines need to be re-evaluated in light of these findings. We suggest SOX9 to be a more suitable biomarker although more biological insight of its role in CRC is needed. In the perspective of targeted therapy, we are of the opinion that inhibition of MAPK/PI3K signaling in CRC is unlikely to be effective. Moreover, the high phospho-ERK1/2 in colon mucosa from NI-WB implies that MAPK signaling possibly serve important functions in normal colonic homeostasis, thus inhibition of MAPK signaling may lead to undesirable consequences. A clearer insight into signaling in human CRC is essential for future therapeutic opportunities.

## Acknowledgements

We would like to thank Professor Daniel Rosenberg of UConn Health, University of Connecticut, USA, for providing details of KRAS mutation status of samples in NCBI GEO series GSE95132. The results shown in Tables S4–S8, Fig. S6B and described in the relevant text are in whole or part based upon data generated by the TCGA Research Network: <https://www.cancer.gov/tcga>. Analysis shown in Fig. S4, Fig. S6A, Table S4 and described in the relevant text are in whole or part based upon data generated by the CPTAC downloaded via LinkedOmics portal (<http://linkedomics.org>). We acknowledge grant funding from National Medical Research Council (NMRC) Singapore grant (OFIRG-0004-2016) and Singapore General Hospital Cancer Peak Research Seed Grant to PYC.

## Conflict of interest

The authors declare no conflict of interest.

## Data accessibility

The data generated in this study are available in Supporting Information Figs. S1–S3, S5. The analyses from public domain data are available in Supporting Information Figs. S4 and S6, Tables S4–S8. These

data were derived from the following resources available in the NCBI GEO at <https://www.ncbi.nlm.nih.gov/geo/> series GSE95132 [24], TCGA Research Network at <https://www.cancer.gov/tcga> via GDC at <https://portal.gdc.cancer.gov> or cBioPortal at <https://www.cbioportal.org> [22,23], and CPTAC COAD dataset downloaded via LinkedOmics portal at <http://linkedomics.org> [21].

## Author contributions

PYC and SHW contributed to the concept, study design, and interpretation of the data. KKL contributed to the acquisition, analysis, and interpretation of the data. CLT and ET contributed to the tissue collection, clinical data, and administration. KKL and PYC drafted the manuscript. KKL, PYC, and SHW contributed to the critical revision of the manuscript. All authors read and approved the final manuscript.

## References

- Sung H, Ferlay J, Siegel RL, Laversanne M, Soerjomataram I, Jemal A, et al. Global cancer statistics 2020: GLOBOCAN estimates of incidence and mortality worldwide for 36 cancers in 185 countries. *CA Cancer J Clin.* 2021;**71**:209–49.
- Singapore Cancer Registry, Annual Registry Report, Trends in Cancer Incidence in Singapore 2010 – 2014. 2015, National Registry of Diseases Office, Singapore: [https://www.nrdo.gov.sg/docs/librariesprovider3/default-document-library/cancer-trends-report-2010---2014\\_web.pdf?sfvrsn=0](https://www.nrdo.gov.sg/docs/librariesprovider3/default-document-library/cancer-trends-report-2010---2014_web.pdf?sfvrsn=0).
- Goyle S, Maraveyas A. Chemotherapy for colorectal cancer. *Dig Surg.* 2005;**22**:401–14.
- Bleiberg H. Adjuvant treatment of colon cancer. *Curr Opin Oncol.* 2005;**17**:381–5.
- Karapetis CS, Khambata-Ford S, Jonker DJ, O'Callaghan CJ, Tu D, Tebbutt NC, et al. K-ras mutations and benefit from cetuximab in advanced colorectal cancer. *N Engl J Med.* 2008;**359**:1757–65.
- Prior IA, Hood FE, Hartley JL. The frequency of Ras mutations in cancer. *Cancer Res.* 2020;**80**:2969–74.
- Misale S, Yaeger R, Hobor S, Scala E, Janakiraman M, Liska D, et al. Emergence of KRAS mutations and acquired resistance to anti-EGFR therapy in colorectal cancer. *Nature.* 2012;**486**:532–6.
- Diaz LA Jr, Williams RT, Wu J, Kinde I, Hecht JR, Berlin J, et al. The molecular evolution of acquired resistance to targeted EGFR blockade in colorectal cancers. *Nature.* 2012;**486**:537–40.
- Chin L, Tam A, Pomerantz J, Wong M, Holash J, Bardeesy N, et al. Essential role for oncogenic Ras in tumour maintenance. *Nature.* 1999;**400**:468–72.
- Rui Y, Wang C, Zhou Z, Zhong X, Yu Y. K-Ras mutation and prognosis of colorectal cancer: a meta-analysis. *Hepatogastroenterology.* 2015;**62**:19–24.
- Huang D, Sun W, Zhou Y, Li P, Chen F, Chen H, et al. Mutations of key driver genes in colorectal cancer progression and metastasis. *Cancer Metastasis Rev.* 2018;**37**:173–87.
- Ottaiano A, Normanno N, Facchini S, Cassata A, Nappi A, Romano C, et al. Study of Ras Mutations' prognostic value in metastatic colorectal cancer: STORIA analysis. *Cancers.* 2020;**12**:1919.
- Stephen AG, Esposito D, Bagni RK, McCormick F. Dragging ras back in the ring. *Cancer Cell.* 2014;**25**:272–81.
- Cox AD, Fesik SW, Kimmelman AC, Luo J, Der CJ. Drugging the undruggable RAS: Mission possible? *Nat Rev Drug Discov.* 2014;**13**:828–51.
- Ostrem JM, Peters U, Sos ML, Wells JA, Shokat KM. K-Ras(G12C) inhibitors allosterically control GTP affinity and effector interactions. *Nature.* 2013;**503**:548–51.
- Rowell CA, Kowalczyk JJ, Lewis MD, Garcia AM. Direct demonstration of geranylgeranylation and farnesylation of Ki-Ras in vivo. *J Biol Chem.* 1997;**272**:14093–7.
- Whyte DB, Kirschmeier P, Hockenberry TN, Nunez-Oliva I, James L, Catino JJ, et al. K- and N-Ras are geranylgeranylated in cells treated with farnesyl protein transferase inhibitors. *J Biol Chem.* 1997;**272**:14459–64.
- Fang JY, Richardson BC. The MAPK signalling pathways and colorectal cancer. *Lancet Oncol.* 2005;**6**:322–7.
- Drosten M, Barbacid M. Targeting the MAPK pathway in KRAS-driven tumors. *Cancer Cell.* 2020;**37**:543–50.
- Xie YH, Chen YX, Fang JY. Comprehensive review of targeted therapy for colorectal cancer. *Signal Transduct Target Ther.* 2020;**5**:22.
- Vasaikar S, Huang C, Wang X, Petyuk VA, Savage SR, Wen B, et al. Proteogenomic analysis of human colon cancer reveals new therapeutic opportunities. *Cell.* 2019;**177**:1035–49.
- Cerami E, Gao J, Dogrusoz U, Gross BE, Sumer SO, Aksoy BA, et al. The cBio cancer genomics portal: an open platform for exploring multidimensional cancer genomics data. *Cancer Discov.* 2012;**2**:401–4.
- Gao J, Aksoy BA, Dogrusoz U, Dresdner G, Gross B, Sumer SO, et al. Integrative analysis of complex cancer genomics and clinical profiles using the cBioPortal. *Sci Signal.* 2013;**6**:1.
- Hanley MP, Hahn MA, Li AX, Wu X, Lin J, Wang J, et al. Genome-wide DNA methylation profiling reveals cancer-associated changes within early colonic neoplasia. *Oncogene.* 2017;**36**:5035–44.

- 25 Grossman RL, Heath AP, Ferretti V, Varmus HE, Lowy DR, Kibbe WA, et al. Toward a shared vision for cancer genomic data. *N Engl J Med*. 2016;**375**:1109–12.
- 26 Afgan E, Baker D, Batut B, van den Beek M, Bouvier D, Cech M, et al. The Galaxy platform for accessible, reproducible and collaborative biomedical analyses: 2018 update. *Nucleic Acids Res*. 2018;**46**:W537–44.
- 27 Love MI, Huber W, Anders S. Moderated estimation of fold change and dispersion for RNA-seq data with DESeq2. *Genome Biol*. 2014;**15**:550.
- 28 Kim D, Langmead B, Salzberg SL. HISAT: a fast spliced aligner with low memory requirements. *Nat Methods*. 2015;**12**:357–60.
- 29 Anders S, Pyl PT, Huber W. HTSeq—a Python framework to work with high-throughput sequencing data. *Bioinformatics*. 2015;**31**:166–9.
- 30 Huang DW, Sherman BT, Lempicki RA. Bioinformatics enrichment tools: paths toward the comprehensive functional analysis of large gene lists. *Nucleic Acids Res*. 2009;**37**:1–13.
- 31 Huang DW, Sherman BT, Lempicki RA. Systematic and integrative analysis of large gene lists using DAVID bioinformatics resources. *Nat Protoc*. 2009;**4**:44–57.
- 32 Reimand J, Kull M, Peterson H, Hansen J, Vilo J. g:Profiler—a web-based toolset for functional profiling of gene lists from large-scale experiments. *Nucleic Acids Res*. 2007;**35**:W193–200.
- 33 Raudvere U, Kolberg L, Kuzmin I, Arak T, Adler P, Peterson H, et al. g:Profiler: a web server for functional enrichment analysis and conversions of gene lists (2019 update). *Nucleic Acids Res*. 2019;**47**:W191–8.
- 34 Ling S, Chang X, Schultz L, Lee TK, Chaux A, Marchionni L, et al. An EGFR-ERK-SOX9 signaling cascade links urothelial development and regeneration to cancer. *Cancer Res*. 2011;**71**:3812–21.
- 35 Attar BM, Atten MJ, Holian O. MAPK activity is down-regulated in human colon adenocarcinoma: correlation with PKC activity. *Anticancer Res*. 1996;**16**:395–9.
- 36 Eggstein S, Franke M, Kutschka I, Manthey G, von Specht BU, Ruf G, et al. Expression and activity of mitogen activated protein kinases in human colorectal carcinoma. *Gut*. 1999;**44**:834–8.
- 37 Park KS, Kim NG, Kim JJ, Kim H, Ahn YH, Choi KY. Differential regulation of MAP kinase cascade in human colorectal tumorigenesis. *Br J Cancer*. 1999;**81**:1116–21.
- 38 Wang Q, Ding Q, Dong Z, Ehlers RA, Evers BM. Downregulation of mitogen-activated protein kinases in human colon cancers. *Anticancer Res*. 2000;**20**:75–83.
- 39 Hoshino R, Chatani Y, Yamori T, Tsuruo T, Oka H, Yoshida O, et al. Constitutive activation of the 41-/43-kDa mitogen-activated protein kinase signaling pathway in human tumors. *Oncogene*. 1999;**18**:813–22.
- 40 Haigis KM, Kendall KR, Wang Y, Cheung A, Haigis MC, Glickman JN, et al. Differential effects of oncogenic K-Ras and N-Ras on proliferation, differentiation and tumor progression in the colon. *Nat Genet*. 2008;**40**:600–8.
- 41 Gulmann C, Sheehan KM, Conroy RM, Wulfkühle JD, Espina V, Mullarkey MJ, et al. Quantitative cell signalling analysis reveals down-regulation of MAPK pathway activation in colorectal cancer. *J Pathol*. 2009;**218**:514–9.
- 42 Yeh JJ, Routh ED, Rubinas T, Peacock J, Martin TD, Shen XJ, et al. KRAS/BRAF mutation status and ERK1/2 activation as biomarkers for MEK1/2 inhibitor therapy in colorectal cancer. *Mol Cancer Ther*. 2009;**8**:834–43.
- 43 Sakakura C, Hagiwara A, Shirahama T, Nakanishi M, Yasuoka R, Fujita Y, et al. Infrequent activation of mitogen-activated protein kinase in human colon cancers. *Hepatogastroenterology*. 1999;**46**:2831–4.
- 44 Schmitz KJ, Wohlschlaeger J, Alakus H, Bohr J, Stauder MA, Worm K, et al. Activation of extracellular regulated kinases (ERK1/2) but not AKT predicts poor prognosis in colorectal carcinoma and is associated with k-ras mutations. *Virchows Arch*. 2007;**450**:151–9.
- 45 Kuno Y, Kondo K, Iwata H, Senga T, Akiyama S, Ito K, et al. Tumor-specific activation of mitogen-activated protein kinase in human colorectal and gastric carcinoma tissues. *Jpn J Cancer Res*. 1998;**89**:903–9.
- 46 Cassano A, Bagala C, Battelli C, Schinzari G, Quirino M, Ratto C, et al. Expression of vascular endothelial growth factor, mitogen-activated protein kinase and p53 in human colorectal cancer. *Anticancer Res*. 2002;**22**:2179–84.
- 47 Lee SH, Lee JW, Soung YH, Kim SY, Nam SW, Park WS, et al. Colorectal tumors frequently express phosphorylated mitogen-activated protein kinase. *APMIS*. 2004;**112**:233–8.
- 48 Nemoto T, Kubota S, Ishida H, Murata N, Hashimoto D. Ornithine decarboxylase, mitogen-activated protein kinase and matrix metalloproteinase-2 expressions in human colon tumors. *World J Gastroenterol*. 2005;**11**:3065–9.
- 49 Perkins G, Lievre A, Ramacci C, Meatchi T, de Reynies A, Emile JF, et al. Additional value of EGFR downstream signaling phosphoprotein expression to KRAS status for response to anti-EGFR antibodies in colorectal cancer. *Int J Cancer*. 2010;**127**:1321–31.
- 50 Lee MS, Menter DG, Kopetz S. Right versus left colon cancer biology: integrating the consensus molecular subtypes. *J Natl Compr Canc Netw*. 2017;**15**:411–9.
- 51 Aggarwal S, Suzuki T, Taylor WL, Bhargava A, Rao RK. Contrasting effects of ERK on tight junction integrity in differentiated and under-differentiated Caco-2 cell monolayers. *Biochem J*. 2011;**433**:51–63.

- 52 Bhat AA, Uppada S, Achkar IW, Hashem S, Yadav SK, Shanmugakonar M, et al. Tight junction proteins and signaling pathways in cancer and inflammation: a functional crosstalk. *Front Physiol.* 2018;**9**:1942.
- 53 Weinstein JN. Drug discovery: cell lines battle cancer. *Nature.* 2012;**483**:544–5.
- 54 Kress TR, Raabe T, Feller SM. High Erk activity suppresses expression of the cell cycle inhibitor p27Kip1 in colorectal cancer cells. *Cell Commun Signal.* 2010;**8**:1.
- 55 Moser AR, Luongo C, Gould KA, McNeley MK, Shoemaker AR, Dove WF. ApcMin: a mouse model for intestinal and mammary tumorigenesis. *Eur J Cancer.* 1995;**31A**:1061–4.
- 56 Jackstadt R, Sansom OJ. Mouse models of intestinal cancer. *J Pathol.* 2016;**238**:141–51.
- 57 Lieu CH, Tan AC, Leong S, Diamond JR, Eckhardt SG. From bench to bedside: lessons learned in translating preclinical studies in cancer drug development. *J Natl Cancer Inst.* 2013;**105**:1441–56.
- 58 Harmston N, Lim JYS, Arques O, Palmer HG, Petretto E, Virshup DM, et al. Widespread repression of gene expression in cancer by a Wnt/beta-Catenin/MAPK Pathway. *Cancer Res.* 2021;**81**:464–75.
- 59 Uhlen M, Fagerberg L, Hallstrom BM, Lindskog C, Oksvold P, Mardinoglu A, et al. Proteomics. Tissue-based map of the human proteome. *Science.* 2015;**347**:1260419.
- 60 Thul PJ, Akesson L, Wiking M, Mahdessian D, Geladaki A, Ait Blal H, et al. A subcellular map of the human proteome. *Science.* 2017;**356**.
- 61 Uhlen M, Zhang C, Lee S, Sjostedt E, Fagerberg L, Bidkhori G, et al. A pathology atlas of the human cancer transcriptome. *Science.* 2017;**357**:6352.
- 62 Jo A, Denduluri S, Zhang B, Wang Z, Yin L, Yan Z, et al. The versatile functions of Sox9 in development, stem cells, and human diseases. *Genes Dis.* 2014;**1**:149–61.
- 63 Aguilar-Medina M, Avendano-Felix M, Lizarraga-Verdugo E, Bermudez M, Romero-Quintana JG, Ramos-Payan R, et al. SOX9 stem-cell factor: clinical and functional relevance in cancer. *J Oncol.* 2019;**2019**:6754040.
- 64 Liu Y, Sethi NS, Hinoue T, Schneider BG, Cherniack AD, Sanchez-Vega F, et al. Comparative Molecular Analysis of Gastrointestinal Adenocarcinomas. *Cancer Cell.* 2018;**33**(721–735):e8.
- 65 Blum A, Wang P, Zenklusen JC. SnapShot: TCGA-Analyzed Tumors. *Cell.* 2018;**173**:530.
- 66 Kopp JL, von Figura G, Mayes E, Liu FF, Dubois CL, Morris JPT, et al. Identification of Sox9-dependent acinar-to-ductal reprogramming as the principal mechanism for initiation of pancreatic ductal adenocarcinoma. *Cancer Cell.* 2012;**22**:737–50.
- 67 Zhou H, Qin Y, Ji S, Ling J, Fu J, Zhuang Z, et al. SOX9 activity is induced by oncogenic Kras to affect

MDC1 and MCMs expression in pancreatic cancer. *Oncogene.* 2018;**37**:912–23.

## Supporting information

Additional supporting information may be found online in the Supporting Information section at the end of the article.

**Fig. S1.** NI-WB of phospho-ERK1/2 and total-ERK1/2 for all 33 matched CRC mucosa (M) and tumor (T) pairs.

**Fig. S2.** NI-WB of phospho-Akt1/2/3 and pan-Akt1/2/3 for all 33 matched CRC mucosa (M) and tumor (T) pairs.

**Fig. S3.** NI-WB of SOX9 and ACTB for all 33 matched CRC mucosa (M) and tumor (T) pairs.

**Fig. S4.** Phospho-ERK1/2 is downregulated in tumor compared to matched mucosa in the CPTAC-COAD phosphoproteome dataset.

**Fig. S5.** Histological structure of matched mucosa with tumors of low or high phospho-ERK1/2.

**Fig. S6.** SOX9 protein upregulation in CRC tumors vs matched mucosa from CPTAC-COAD and SOX9 mRNA upregulation in KRAS mutant vs WT CRC tumors from TCGA Pan Cancer Atlas.

**Table S1.** Clinico-pathological characteristics of fresh frozen tumor and matched mucosa samples.

**Table S2.** Primers used for PCR amplification and sequencing of KRAS.

**Table S3.** Primary and secondary antibodies and their dilutions in NI-WB.

**Table S4.** Number of CRC tumor-matched mucosa pairs and their respective KRAS and BRAF mutation status retrieved from TCGA and CPTAC.

**Table S5.** The number of upregulated and downregulated genes from the TCGA and NCBI GEO series GSE95132 datasets mapped in DAVID and g:Profiler.

**Table S6.** MAPK-related GO : BP, KEGG and REACTOME terms associated with upregulated (A) and downregulated (B) genes in both TCGA (KRAS WT and mutant Tumors vs Matched Mucosa) and NCBI GEO series GSE95132 (Tumour vs Mucosa and ACFs vs NCs).

**Table S7.** PI3K/Akt-related GO : BP, KEGG and REACTOME terms associated with upregulated genes (A) and downregulated genes (B) in both TCGA (KRAS WT and mutant tumors vs matched mucosa) and NCBI GEO series GSE95132 (Tumour vs Mucosa and ACFs vs NCs).

**Table S8.** Differential Expression of SOX9 from TCGA and NCBI GEO series GSE95132 transcriptome data of tumor compared to matched mucosa, or aberrant crypt foci compared to normal crypts.